

Cross-Flow VIV-Induced Fatigue Damage of Deepwater Steel Catenary Riser at Touch-Down Point*

WANG Kun-peng (王坤鹏), TANG Wen-yong (唐文勇)
and XUE Hong-xiang (薛鸿祥)¹

*State Key Laboratory of Ocean Engineering, Shanghai Jiao Tong University,
Shanghai 200240, China*

(Received 11 May 2012; received revised form 4 March 2013; accepted 28 June 2013)

ABSTRACT

A prediction model of the deepwater steel catenary riser VIV is proposed based on the forced oscillation test data, taking into account the riser-seafloor interaction for the cross-flow VIV-induced fatigue damage at touch-down point (TDP). The model will give more reasonable simulation of SCR response near TDP than the previous pinned truncation model. In the present model, the hysteretic riser-soil interaction model is simplified as the linear spring and damper to simulate the seafloor, and the damping is obtained according to the dissipative power during one periodic riser-soil interaction. In order to validate the model, the comparison with the field measurement and the results predicted by Shear 7 program of a full-scale steel catenary riser is carried out. The main induced modes, mode frequencies and response amplitude are in a good agreement. Furthermore, the parametric studies are carried out to broaden the understanding of the fatigue damage sensitivity to the upper end in-plane offset and seabed characteristics. In addition, the fatigue stress comparison at TDP between the truncation riser model and the present full riser model shows that the existence of touch-down zones is very important for the fatigue damage assessment of steel catenary riser at TDP.

Key words: *VIV; steel catenary riser; touch-down point; riser-soil interaction; fatigue damage*

1. Introduction

Steel catenary riser (SCR) is a kind of long slender structure hanging freely from the seabed to the floating production system, and its application has increased extensively in the past few years with oil and gas production moving to the deep and ultra-deep water. In the ocean current, SCR is subject to vortex induced vibration (VIV), and if the vortex shedding frequency is locked in the structure frequency, the VIV response will amplify, which is potential to result in fatigue damage failure. Therefore, it is vital for reasonable SCR design to estimate the VIV-induced fatigue damage.

In recent years, the VIV prediction of an SCR has always been a hot issue that many researchers are interest in, and some meaningful studies are carried out. Narakorn *et al.* (2009) used the van der Pol wake oscillator to model the unsteady hydrodynamic force associated with cross-flow and in-line vibration, besides, the hydrodynamic model was modified to capture the effect of the varying initial curvature and to describe the space-time fluctuation of lift and drag force. A single wake oscillator and

* The work was financially supported by the National Natural Science Foundation of China (Grant No. 51009089), and the Specialized Research Fund for the Doctoral Program of Higher Education of China (Grant No. 20100073120017).

¹ Corresponding author. E-mail: hongxiangxue@sjtu.edu.cn

a vortex tracking model were attached with each element by Mark Chang and Isherwood (2003) to construct a time domain VIV analysis method, by which an SCR was analyzed in consideration of the platform heave motion. Gao and Zong (2011) used the forced oscillation test data as the hydrodynamic coefficient to study the VIV-induced fatigue damage of an SCR under frequency domain. Rao *et al.* (2011) studied the sensitivity of the root mean square (RMS) and mode number of the VIV response of an SCR to the current profile. The studies stated before often used the truncation model freely hanging with rotation stiffness at TDP, the same way even used in the commercial VIV prediction software, Shear7 (Vandiver and Li, 2005) and VIVANA (Larsen and Vikestad, 2005). One of the critical issues in an SCR design is to estimate the fatigue life at TDP. However, truncation model could not account for the riser-seafloor interaction, which would cause unreasonable results.

Owing to its importance and complexity, the riser-seafloor interaction is paid much attention by the offshore industry, and some projects to study its mechanism using full scale SCR were carried out successively, such as STRIDE JIP launched by 2H Offshore Engineering Ltd (Bridge and Laver, 2004), and CARISIMA JIP launched by ExxonMobile *et al.* (Leira and Passano, 2004). According to the riser-seafloor interaction process described by Bridge and Laver (2004), Aubeny *et al.* (2006) proposed the nonlinear hysteretic p - y curve model. Based on this model, a series of work were carried out to study the wave induced response and fatigue of SCR at TDP (Randolph and Quiggin, 2009; Nakhaee and Zhang, 2010; Wang *et al.*, 2011), whereas the study for VIV to account for the riser-soil interaction by using this model is still a new research field.

In this paper, the VIV prediction model considering the riser-seafloor interaction is developed in frequency domain. The cylinder forced oscillation test data are used to model the hydrodynamic force. The seabed is simplified as the spring and damping based on the equivalent power dissipation during one periodic oscillation following the full loop depicted in the hysteretic riser-seafloor interaction model. To determine the maximum penetration of the hysteretic model at each position, beam-spring model is applied to form an initial trench, which is assumed to remain constant during the analysis. Validation is performed by the comparison of predicted mode frequencies and amplitude with those obtained from field measurement and Shear7. Then parametric analyses are carried out to study the sensitivity of the fatigue damage at TDP to the seabed stiffness, clay suction and upper end in-plane offset, and at last, some useful conclusions are obtained. It should be noted that the traditional truncation model could not well achieve above ones due to not applying zero displacement at TDP.

2. Riser-Seafoor Interaction Model

Although the mechanism of riser-seafloor interaction is complex, some particular phenomena, such as clay suction and seabed degradation, are obtained through full scale SCR test, and some useful models are proposed. The nonlinear hysteretic riser-seafloor interaction model including five subsections formulated by Aubeny and Biscontin (2009) that well capture the mobilization and release the clay suction will be used in this study. The sketch is shown in Fig. 1. For the completeness, each subsection will be briefly described below.

The backbone curve l_1 is approximate by Eq. (1):

$$P = N_p D (S_0 + S_g |y|), \tag{1}$$

where S_0 and S_g are mudline shear strength and shear strength gradient, respectively; D is the outer diameter of the riser; $|y|$ is the riser penetration; N_p is the non-dimensional bearing factor, expressed as follows:

$$N_p = a (|y|/D)^b, \tag{2}$$

where a and b are test parameters and equal to 6.7 and 0.254, respectively.

The elastic rebound curve l_2 is described by Eqs. (3)–(5):

$$P = P_1 + (|y| - |y|_1) \left/ \left(\frac{1}{k_0} - \frac{|y| - |y|_1}{(1 + \omega) P_1} \right) \right.; \tag{3}$$

$$|y|_2 = |y|_1 - \frac{(1 + \lambda) P_1}{k_0} \frac{1 + \varphi}{\lambda - \varphi}; \tag{4}$$

$$P_2 = -\varphi P_1, \tag{5}$$

where P_1 represents the seabed resistance associated with the penetration of $|y|_1$ at Point 1, which is governed by the backbone curve; P_2 and $|y|_2$ are the maximum clay suction and related penetration at Point 2, respectively; k_0 defines the initial slope of hyperbola; ω and φ are non-dimensional parameters; λ is equal to 0.433 and φ connects the maximum resistance and the maximum suction.

The partial riser-soil separation curve l_3 is given by Eqs. (6) and (7):

$$P = \frac{P_2}{2} + \frac{P_2}{4} \left[3 \left(\frac{|y| - (|y|_2 + |y|_3)/2}{(|y|_2 - |y|_3)/2} \right) - \left(\frac{|y| - (|y|_2 + |y|_3)/2}{(|y|_2 - |y|_3)/2} \right)^3 \right]; \tag{6}$$

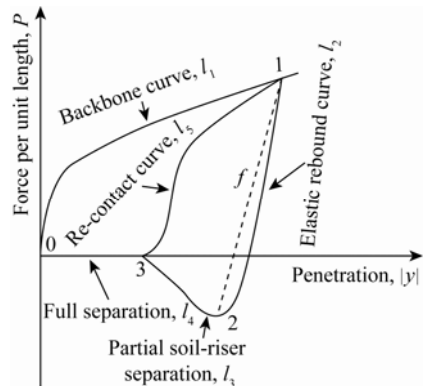
$$|y|_3 = |y|_2 - \gamma (|y|_1 - |y|_2), \tag{7}$$

where γ is a non-dimensional parameter taken to be $|y|_2/(|y|_1 - |y|_2)$ in this paper.

Equation for re-contact curve l_5 is expressed as:

$$P = \frac{P_1}{2} + \frac{P_1}{4} \left[3 \left(\frac{|y| - (|y|_1 + |y|_3)/2}{(|y|_1 - |y|_3)/2} \right) - \left(\frac{|y| - (|y|_1 + |y|_3)/2}{(|y|_1 - |y|_3)/2} \right)^3 \right]. \tag{8}$$

Fig. 1. Typical riser-soil interaction model.



In order to obtain the penetration $|y|_1$ at each position of touchdown zone (TDZ), the beam-spring model proposed by Aubeny *et al.* (2006) is used in this paper, which is shown in Fig. 2 and formulated as:

$$EI \frac{d^4 |y|}{dx^4} = W - P_b, \quad (9)$$

where E is young's modulus, I is the moment of inertia, W is the riser wet weight per unit length, and P_b is the seafloor resistance per unit length corresponding to the backbone curve.

The finite difference method is used to solve Eq. (9) when the boundary condition of the beam end B and the maximum penetration $|y|_{\max}$ are given. Owing to the non-linearity of the p - y curve, for a given contact θ_A at touch-down point, the analysis procedure must iterate until the value of $|y|$ at the beginning of iteration lies sufficiently close to that updated at the end of the iteration calculation. By changing θ_A and repeating above iteration to achieve the targeted $|y|_{\max}$, an initial riser configuration at TDZ can be obtained.

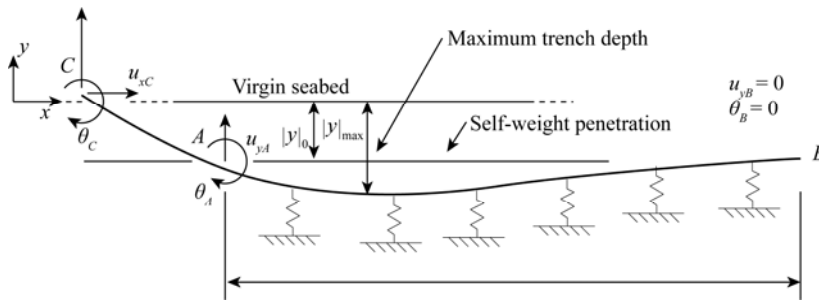


Fig. 2. Beam-spring model.

Owing to the non-linearity of the hysteretic riser-seafloor interaction model making it unfeasible in frequency domain directly, it is simplified as spring and damping in this paper. The spring stiffness is determined by the slope of line f shown in Fig. 1, and damping value can be obtained by Eq. (10) under the assumption that the dissipated power in one periodic oscillation is equivalent to the area enclosed by the hysteretic model.

$$c_{\text{soil}} = \frac{4\Pi_i^k}{\pi\omega_k \left(|y|_{1,i}\right)^2}, \quad (10)$$

where Π_i^k is the dissipated power in one period at point i due to the oscillation of mode k , ω_k is the circular frequency of mode k , and $|y|_{1,i}$ is the maximum penetration at point i .

3. VIV Prediction Model

This paper study the cross-flow VIV of SCR induced by the current perpendicular to the plane,

which is shown in Fig. 3. Partial differential equation that governs the riser motion and the distributed fluid excitation are presented:

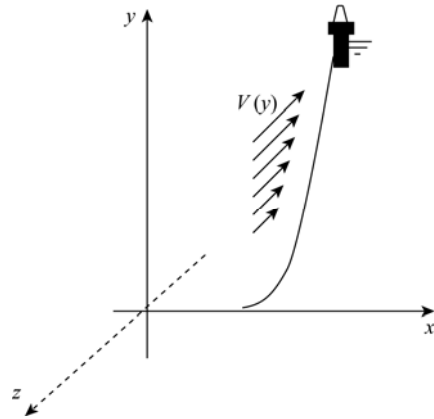
$$(\rho + m_a) \frac{\partial^2 x(y,t)}{\partial t^2} + c \frac{\partial x(y,t)}{\partial t} + EI \frac{\partial^4 x(y,t)}{\partial y^4} - T \frac{\partial^2 x(y,t)}{\partial y^2} = F(y,t) + W + F_B, \quad (11)$$

where ρ is the mass per unit length; m_a is the added mass; EI is the flexural stiffness; T is the axial force; c is the damping coefficient including structure damping c_s , hydrodynamic damping c_f (Venugopal, 1996) and soil damping c_{soil} ; W and F_B are the riser weight and buoyancy per unit length, respectively; $F(y,t)$ is the lift force given by:

$$F(y,t) = \frac{1}{2} \rho_f D V^2(y) C_L(y, \omega_k) \sin(\omega_k t), \quad (12)$$

where ρ_f is the fluid density, and C_L is the lift coefficient obtained from the cylinder forced oscillation test by Gopalkrishnan (1993).

Fig. 3. Sketch of steel catenary riser.



According to the mode superposition theory, the displacement can be expressed as:

$$x(y,t) = \sum_k X_k(y) Q_k(t), \quad (13)$$

where $X_k(y)$ and $Q_k(t)$ are the normalized modal shape function and coordinate function of mode k , respectively. In this study, the natural frequency and mode shape are obtained using FE software, ABAQUS.

Let the modal velocity of mode k be

$$\dot{Q}_k(t) = A_k \omega_k \sin(\omega_k t), \quad (14)$$

where A_k is the modal displacement amplitude of riser for mode k . It is assumed that, for this mode, the input and output power are in balance. Then the following expression is obtained:

$$\frac{A_k}{D} = \frac{\frac{1}{2} \int_{L_f} \rho_f V^2(y) C_L(y, \omega_k) |X_k(y)| dy}{\int_{L-L_f-L_{soil}} c_f(y) X_k^2(y) \omega_k dy + \int_L c_s(y) X_k^2(y) \omega_k dy + \int_{L_{soil}} c_{soil}(y) X_k^2(y) \omega_k dy}, \quad (15)$$

where L , L_f and L_{soil} represent the length of the whole riser, the power-in region, and the touch-down zone, respectively.

In the program, an initial value is assigned to the lift coefficient. The iteration calculation is performed with the updated lift force and damping, until the convergence is reached for A_k/D .

4. Validation of the VIV Prediction Program

Nicholas and Bridge (2007) detailed the measured results of cross-flow VIV of an SCR for the gas production in the Gulf of Mexico with the depth of 1000 m, showing a good comparison with that obtained from Shear7 by using pinned-pinned model. Fig. 4 gives the sketch of SCR, and Fig. 5 is the associated current profile (Willis, 2001).

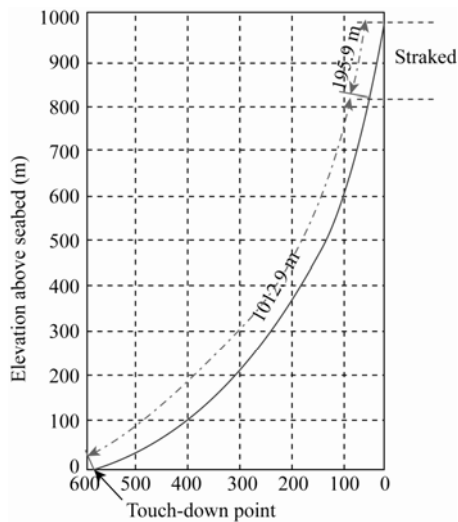


Fig. 4. Sketch of the monitored steel catenary riser.

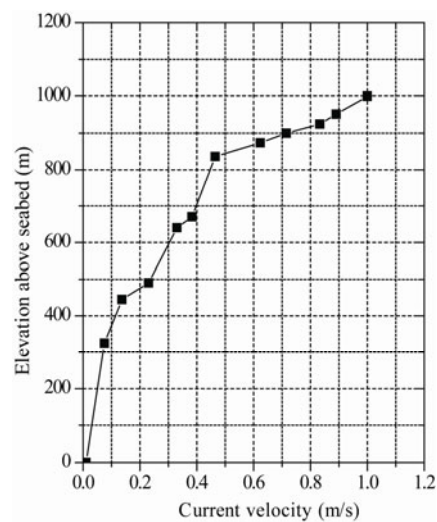


Fig. 5. Current profile.

To study the influence of the existence of TDZ, a truncation model (similar to the Shear7 prediction model) and a full model including TDZ with the length of 186 m are created in the present program. In the full model, the median range of soil classification in the Gulf of Mexico is used: $S_0=2.6$ kPa, $S_g=1.25$ kPa/m (Willis and West, 2001). Table 1 presents the parameters of VIV prediction model.

Table 1 Parameters of VIV prediction model

Parameters	values
Length (m)	1394.8
Outer diameter (m)	0.3048
Inner diameter (m)	0.2728
Mass (kg/m)	114
Top tension (N)	4.78×10^5
Strake region added mass coefficient	2.0
non-strake region added mass coefficient	1.0
Strake lift coefficient reduction factor	0.25
Structural damping coefficient	0.005

The natural frequencies of SCR obtained from three different methods are presented in Table 2. Relative to the field measurement, the Shear7 model and the present models give slightly higher prediction results. Additionally, a good comparison of the predicted frequency between the truncation model and the full model indicates that there is almost no influence of TDZ on the natural frequency of this SCR. Fig. 6 gives the amplified modal shape of Modes 16–18, illustrating that the two models are almost the same at the catenary part, whereas show significantly different near TDP.

Table 2 Response frequency of steel catenary riser

Modes	Measured frequency (Hz)	Shear7 prediction frequency (Hz)	Present program prediction frequency (Hz)	
			Truncation model	Full model
16	0.270	0.288	0.282	0.281
17	0.290	0.310	0.303	0.303
18	0.310	0.332	0.324	0.323

Next, the amplitude of vibration is compared since it determines whether the present program can predict the VIV fatigue damage accurately. The modal displacement amplitudes are given in Table 3, where the difference smaller than 10% can be seen for Modes 17 and 18, but the present program predicts Mode 16 amplitude by 4%. A comparison between the two model results obtained from the present program shows that, as well as the natural frequency, the oscillation amplitude will not be affected by the existence of TDZ.

Table 3 Dominant mode amplitude of the steel catenary riser

Modes	Measurement amplitude (m)	Shear7 prediction amplitude (m)	Present program prediction amplitude (m)	
			Truncation model	Full model
16	0.0310	0.0340	0.0323	0.0320
17	0.0160	0.0240	0.0140	0.0145
18	0.0180	0.0170	0.0168	0.0168

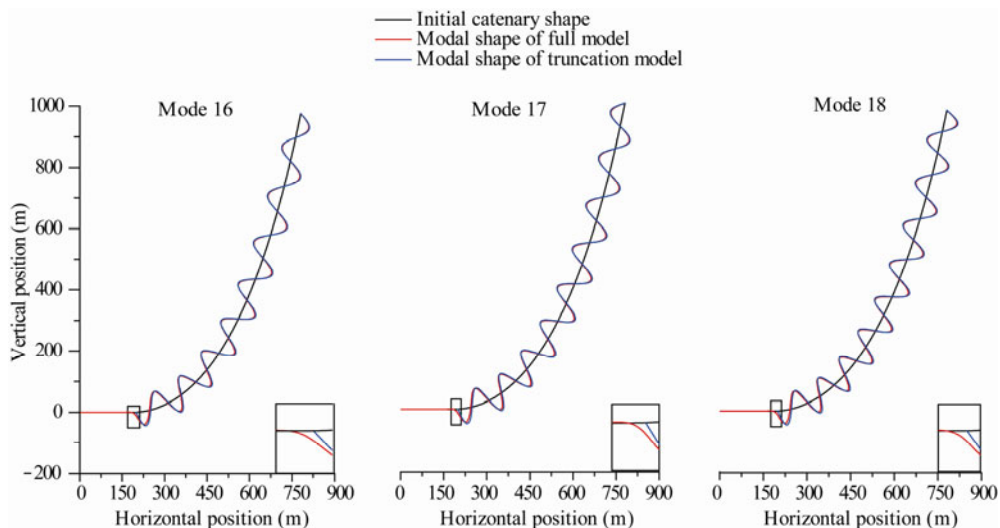


Fig. 6. Modal shape of the steel catenary riser.

5. Fatigue Life Prediction at TDP

5.1 S-N Curve Method

The S-N approach has been widely used to solve the fatigue problem. To obtain the fatigue life of SCR at TDP, it is assumed that the material behavior could be well represented by D curve specified in DNV-RP-C203 (DNV, 2005) expressed as:

$$N = A \left[\left(\Delta S \cdot SCF \cdot \left(t / t_{\text{ref}} \right)^k \right) \right]^{-m}, \quad (16)$$

where N is the permissible number of cycles with the applied stress range ΔS in MPa; SCF is the stress concentration factor, equal to 1.0; A and m are the material constants; t/t_{ref} is the thickness correction factor, and the reference thickness t_{ref} is equal to 25 mm.

The multi-mode VIV-induced stress range can be combined by the square root of the sum square (SRSS) approach and the cycle counting frequency is taken to be the weighted SRSS frequency (Xue et al., 2009):

$$\Delta S = \sqrt{\sum_k (\Delta S_k)^2}, \quad f = \sqrt{\sum_k \left(f_k \frac{\Delta S_k}{\Delta S} \right)^2}, \quad (17)$$

where ΔS_k and f_k are the effective stress range and natural frequency of mode k . The mean stress is taken into account to obtain ΔS_k by using the Goodman method:

$$\Delta S_k = \frac{S_b \Delta S_{c,k}}{S_b - |S_{m,k}|}, \quad (18)$$

where S_b is the strength limit of material, $S_{c,k}$ is the stress range before mean stress correction, and $S_{m,k}$ is the mean stress.

Then according to the S-N approach, the fatigue life can be expressed as follows:

$$T_f = \frac{D_f A}{f [SCF \cdot \Delta S]^m}, \quad (19)$$

where D_f is the fatigue damage accumulation when fatigue failure occurs. In this study, D_f is set to be 1.0.

5.2 Fatigue Sensitivity Analysis and Discussion

5.2.1 Effect of Linearly Uniform Seafloor Stiffness on the Fatigue Life at TDP

To simplify the analyses, the seafloor is first simulated by linear spring with uniform stiffness along TDZ. The annual fatigue damage along SCR is predicted with seabed stiffness of 200 kN/m, as shown in Fig. 7. The result indicates that TDP is a critical position prone to fatigue failure; at the other part of TDZ from 0 to 150 m, fatigue damage is very little. Fig. 8 illustrates the fatigue life at TDP with different linear seafloor stiffness, including 100 kN/m, 150 kN/m, 200 kN/m, 250 kN/m, and 300 kN/m. The result shows that the linear stiffness has a significant influence on the fatigue life at TDP, and the higher linear stiffness predicts lower fatigue life.

5.2.2 Effect of Upper End in-Plane Offset on the Fatigue Life at TDP

In the sea, the current, wind and mean drift wave force may result in the upper end offset of an SCR connected with the platform. This has a significant influence on the position of TDP. By horizontally translating the upper end, the study obtains the SCR shape near TDP, as shown in Fig. 9. The varied position of TDP is destined to change its fatigue life. Fig. 10 gives the fatigue life of SCR at TDPs associated with different upper end in-plane static offset. It shows the increment (decrement) of fatigue life with positive (negative) offset along the x-axis. Fig. 11 denotes that, although the positive offset is in favor of the TDP, it obviously increases the upper end tension, which may be fatal for the flexible joint connecting the platform and SCR.

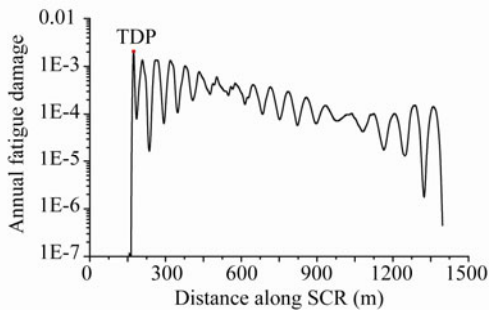


Fig. 7. Fatigue damage along SCR with seabed stiffness of 200 kN/m.

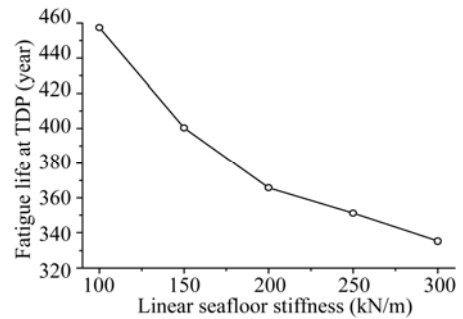


Fig. 8. Fatigue life at TDP of SCR with different linear seafloor stiffness.

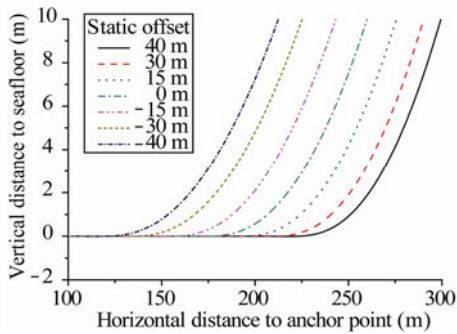


Fig. 9. Sketch of SCR near TDP with different static offset.

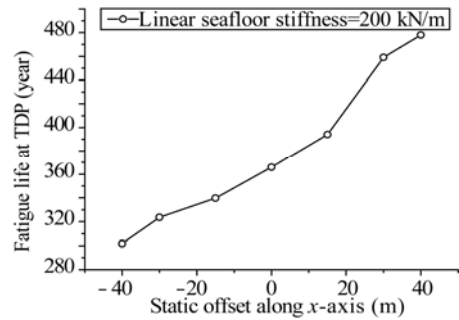
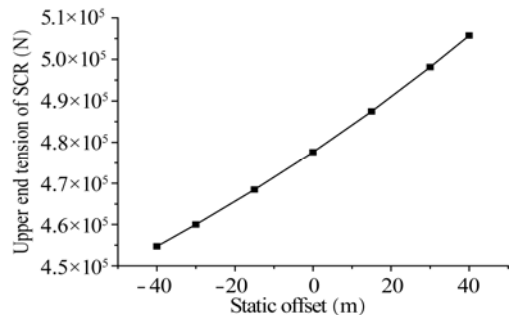


Fig. 10. Fatigue life at TDP with different static offset.

Fig. 11. Upper end tension of SCR with different static offset.



5.2.3 Effect of Mudline Shear Strength and Shear Strength Gradient on Fatigue Life at TDP

Compared with the linear spring with constant stiffness, the linear spring and damping equivalent

to the hysteretic model gives more detail description about riser-seafloor interaction. The seafloor strength is reflected by the mudline shear strength and the shear strength gradient. To study their influence on the fatigue life at TDP, a series of fatigue analyses are performed for the SCR. In these analyses, an initial trench is determined by the beam-spring model with the maximum penetration y_{\max} of 2 riser diameters.

Fatigue analyses are first undertaken for this case by using a constant shear strength gradient, with a range of values of the mudline shear strength. The predicted fatigue life is shown in Fig. 12, as a function of the mudline shear strength. It is seen that the effect is significant, and the higher mudline shear strength, corresponding to the stiffer seabed, gives a lower fatigue life. In addition, its effects on fatigue life decreases obviously with the increasing mudline shear strength.

Further fatigue analyses are undertaken, but this time with a varying shear strength gradient and constant mudline shear strength. Fig. 13 gives the predicted fatigue life. With the mudline shear strength, the higher shear strength gradient predicts a lower fatigue life.

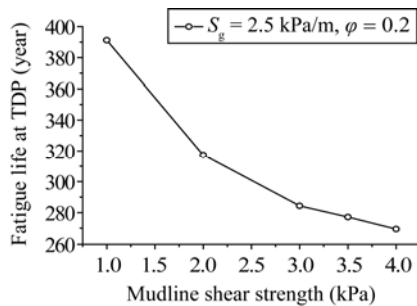


Fig. 12. Effect of mudline shear stiffness on TDP's fatigue life.

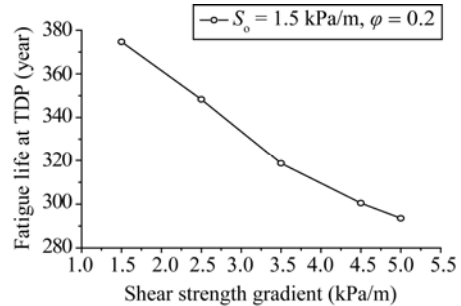


Fig. 13. Effect of shear stiffness gradient on TDP's fatigue life.

The previous models often use pinned-pinned truncation model to predict the VIV response of an SCR, applying the fixed constrain and certain rotation stiffness at TDP. As an improvement, the full model proposed in this paper considers the riser-seafloor interaction. In order to study the difference between the two models, the following analyses are performed.

Fatigue life at TDP as a function of rotation stiffness is shown in Fig. 14, where the higher rotation stiffness gives a lower fatigue life. Truncation model with the rotation stiffness of $2.4E6$ Nm/rad at TDP predicts the same fatigue life using the full model with the mudline shear strength of 1 kPa and the shear strength gradient of 2.5 kPa/m. However, under these boundary conditions, the mean stress and stress range before the mean stress correction are different, approximate to 77.6 MPa and 4.93 MPa for the truncation model, but for the full model about 46 MPa and 5.91 MPa.

From the above discussion, it can be concluded that the higher rotation stiffness corresponds to the stiffer seabed as well as the higher mudline shear strength and shear strength gradient, but due to different boundary conditions, the stress response of the two models at TDP is obviously different. As shown in Fig. 15, for the full model, the mean stress almost remains constant as the mudline shear strength increases, but for the truncation model, it substantially increases as the rotation stiffness

increases. Figs. 16 and 17 give the stress range before and after the mean stress correction, respectively. It can be seen that the mean stress of the truncation model contributes more to the effective stress range than the full model.

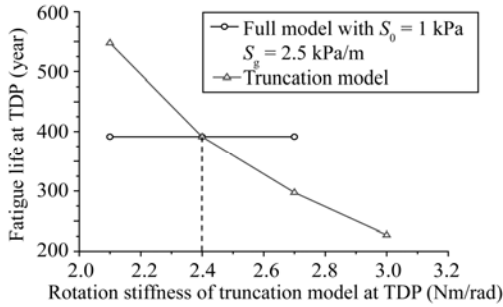


Fig. 14. Fatigue life of the truncation model at TDP.

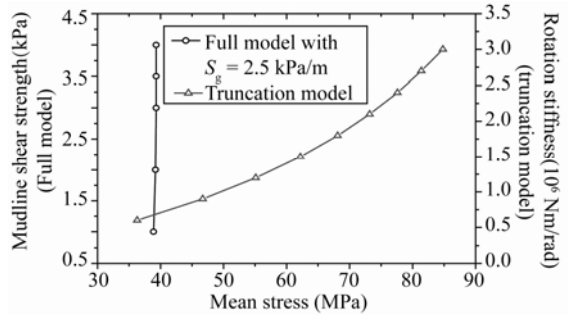


Fig. 15. Mean stress comparison.

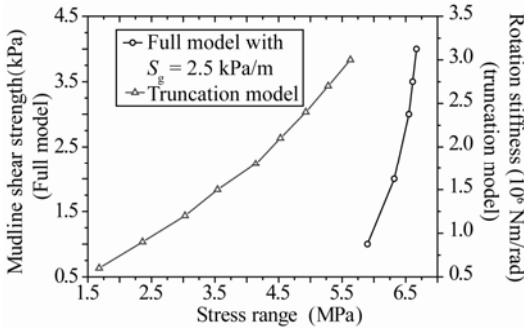


Fig. 16. Comparison of stress range after mean stress correction.

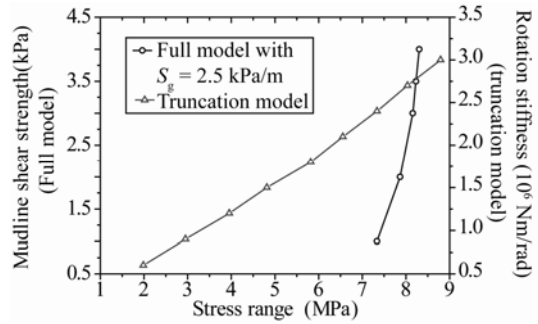
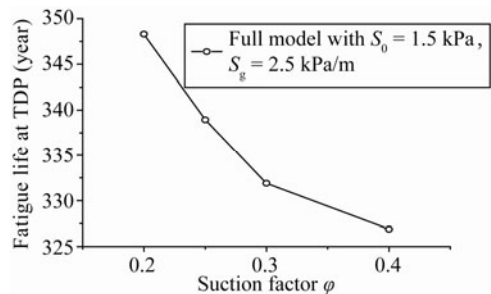


Fig. 17. Comparison of effective stress range before mean stress correction.

5.2.4 Effect of Clay Suction on Fatigue Damage at TDP

The clay suction will appear when the catenary riser moves upwards. To study its effect on the fatigue damage near TDP, fatigue analyses with a range of values of suction factor ϕ are undertaken by use of the full model. In these analyses, the mudline shear strength and shear strength gradient are set to be 1.5 kPa and 2.5 kPa/m, respectively, and the maximum depth y_{max} of the trench is set to be 2 times the riser diameter. The effect of suction factor on the fatigue life at TDP is given in Fig. 18, which shows that the fatigue life decreases with the increasing clay suction.

Fig. 18. Effect of seabed suction on TDP's fatigue life.



6. Conclusions

This paper presents a relatively reasonable VIV prediction model considering the riser-soil interaction to predict the fatigue damage at TDP of SCR. Validation is performed by the comparison of the amplitude and frequency of the main induced modes obtained from the field measurement and the calculation of the truncation SCR model and the full SCR model by using the present program. The full model is then used to carry out the parametric analyses to study the effect of the seafloor characteristics and upper end in-plane offset on the fatigue life at TDP, and the comparison is also performed with the truncation model with regards to the stress range and the fatigue life. From the above studies, the following conclusions can be drawn:

(1) Owing to the comparison with the practical measurement, the present program can simulate the VIV response of SCR reasonably. The existence of TDZ almost has no influence on the natural frequency and the response amplitude, but on the modal shape obviously near TDP. As accounting for more realistic riser-soil interaction, it contributes to a more reasonable fatigue life prediction at TDP.

(2) As the linear seafloor stiffness increases, the fatigue life decreases obviously. Therefore, it is essential to accurately determine the seafloor strength for an SCR design.

(3) The upper end in-plane static offset will change the position of TDP, and the TDP associated with the positive offset along x -axis has a higher fatigue life than that associated with the negative offset. However, the positive offset will give a large upper end tension, which can result in the damage of flexible joint. Therefore, the selection of the static position of SCR should balance the fatigue life at TDP and the capacity of flexible joint.

(4) The higher mudline shear strength and shear strength gradient in the full model give a lower predicted fatigue life, similar to the higher rotation stiffness applied at TDP in the truncation model. However, there are some differences between the two models. With applying zero displacement, the stress response of the truncation model at TDP is obviously different from the full model. The truncation model will have a lower stress range but higher mean stress when the fatigue life of the two models at TDP is the same. As the mudline shear strength and shear strength gradient increase, the stress range increases with almost constant mean stress, but for the truncation model, both the mean stress and stress range increase as the rotation stiffness increases.

(5) The clay suction has a significant effect on the fatigue life at TDP, and a larger suction may result in a lower fatigue life.

In conclusion, the full SCR model in VIV prediction can reflect some special riser-seafloor interaction phenomena, such as clay suction, and also can simulate the seabed stiffness closer to the practical situation compared with the truncation model, so it will be in favor of more reasonable fatigue life prediction of an SCR at TDP.

References

- Aubeny, C. P., Biscontin, G. and Zhang, J., 2006. *Seafloor Interaction with Steel Catenary Risers*, Report, Texas: Texas A&M University.

- Aubeny, C. P. and Biscontin, G., 2009. Seafloor-riser interaction model, *Int. J. Geomech.*, ASCE, **9**(3): 133–141.
- Bridge, C. and Laver K., 2004. Steel catenary riser touchdown point vertical interaction models, *Offshore Technology Conference*, Houston, Texas, USA, OTC 16628.
- DNV, 2005. *Fatigue Design of Offshore Steel Structures*, DNV-RP-C203, Norway.
- Gao, Y. and Zong, Z., 2011. Numerical prediction of fatigue damage in steel catenary riser due to vortex-induced vibration, *Journal of Hydrodynamics*, **23**(2): 154–163.
- Gopalkrishnan, R., 1993. *Vortex Induced Forces on Oscillating Bluff Cylinders*, Department of Ocean Engineering, MIT, Cambridge, USA.
- Larsen, C. M. and Vikestad, K., 2005. *VIVANA-Theory Manual (Version 3.4)*, Norwegian Marine Technology Research Institute, Trondheim, Norway.
- Leira, B. J. and Passano, E., 2004. Analysis guidelines and application of a riser-soil interaction model including trench effects, *Proc. 23rd Int. Conf. Offshore Mech. Arctic Eng. (OMAE2004)*, British, Canada, 51527.
- Mark Chang, S. H. and Isherwood, M., 2003. Vortex-induced vibrations of steel catenary risers and steel offloading lines due to platform heave motions, *Offshore Technology Conference*, Houston, Texas, U.S.A., OTC 15106.
- Nakhaee, A. and Zhang, J., 2010. Trenching effects on dynamic behavior of a steel catenary riser, *Ocean Eng.*, **37**(2–3): 277–288.
- Narakorn, S., Marian, W. and Patrick, O. B., 2009. Reduced-order modeling of vortex-induced vibration of catenary riser, *Ocean Eng.*, **36**(17–18): 1404–1414.
- Nicholas, M. D. and Bridge, C., 2007. Measured VIV response of a deepwater SCR, *Proc. 17th Int. Offshore Polar Eng. Conf. (ISOPE2007)*, Lisbon, Portugal, JSC-473.
- Randolph, M. and Quiggin, P., 2009. Non-linear hysteretic seabed model for catenary pipeline contact, *Proc. 28th Int. Conf. Ocean, Offshore Arctic Eng. (OMAE2009)*, Honolulu, Hawaii, 79259.
- Rao, Z. B., Fu, S. X. and Yang, J. M., 2011. Vortex-induced vibration analysis of steel catenary riser. *J. Ship Mech.*, **15**(3): 245–258.
- Vandiver, J. K. and Li, L., 2005. *SHEAR7 V4.4 Program Theoretical Manual*, Massachusetts Institute of Technology, Cambridge, Massachusetts, USA.
- Venugopal, M., 1996. *Damping and Response of a Flexible Cylinder in a Current*, Department of Ocean Engineering, MIT, Cambridge, USA.
- Wang, K. P., Xue, H. X. and Tang, W. Y., 2011. Dynamic response analysis of deepwater steel catenary riser based on the seabed-suction and stiffness-degradation model, *Journal of Shanghai Jiaotong University*, **45**(4): 585–589. (in Chinese)
- Willis, N., 2001. STRIDE PROJECT–Steel Riser in Deepwater Environments–Recent Highlights, *Proc. 24th Deepwater and Ultra Deepwater Riser Conference*, 2H Offshore LTD.
- Willis, N. R. T. and West, P. T. J., 2001. Interaction between deepwater steel catenary riser and a soft seabed: Large scale sea trials, *Proceedings of Offshore Technology Conference*, Houston, USA, OTC 13113.
- Xue, H. X., Tang, W. Y. and Zhang, S. K., 2009. Simplified model for evaluation of VIV-induced fatigue damage of deepwater marine risers, *Journal of Shanghai Jiaotong University (Science)*, **14**(4): 435–442.